# A Novel Robust Harmonic Injection Method for Single-Switch Three-Phase Discontinuous-Conduction-Mode Boost Rectifiers

Yungtaek Jang, *Member, IEEE,* and Milan M. Jovanović, *Senior Member, IEEE*

***Abstract*— This paper describes a new robust low-cost harmonic-injection method for single-switch three-phase discontinuous-conduction-mode (DCM) boost rectifiers. In the proposed method, a periodic voltage is injected in the control circuit to vary the duty cycle of the rectifier switch within a line cycle so that the fifth-order harmonic of the input current is reduced to meet the IEC555-2 requirement. Since the injected voltage signal, which is proportional to the inverted ac component of the rectified three-phase line-to-line input voltages, is employed, the injected duty-cycle variations are naturally synchronized with the three-phase line-to-neutral input voltages. In addition, the injected harmonic signal naturally contains desirable higher order harmonics, such as sixth, twelfth, eighteenth, etc., which are more effective in improving total harmonic distortions (THD's) than harmonic-injection methods based on the sixth-order harmonic only.**

***Index Terms*— Boost converter, discontinuous conduction mode, harmonic injection, power factor correction, three-phase rectifier.**

## I. Introduction

THE discontinuous-conduction-mode (DCM) pulsewidth-modulated (PWM) high-power-factor boost rectifier for three-phase applications was introduced and analyzed in [1]. The major advantages of this rectifier are that its input-current waveshape automatically follows the input-voltage waveshape and that it can achieve extremely high efficiencies because the reverse-recovery-related losses of the boost diode are eliminated. However, if the rectifier is implemented with the conventional low-bandwidth output-voltage feedback control at a constant switching frequency, which keeps the duty cycle of the switch constant during a rectified line period, the rectifier input current exhibits a relatively large fifth-order harmonic. As a result, at power levels above 5 kW, the fifth-order harmonic imposes severe design, performance, and cost tradeoffs in order to meet the maximum permissible harmonic-current levels defined by the IEC555-2 document [2]. Namely, to meet the IEC555-2 specifications at input-power levels above 5 kW, the DCM boost rectifier must be designed with the output voltage much higher than the peak of the input voltage [3]. Inevitably, such designs require higher voltage-rated switches, which are more expensive and usually have more losses than their counterparts with lower voltage ratings. Generally, to reduce the fifth-order harmonic and to improve THD's of the input currents, the duty cycle of the rectifier switch needs to be properly modulated during a rectified line period instead of being kept constant.

Recently, a number of duty-cycle modulation techniques for the DCM boost rectifier have been introduced to reduce the fifth-order harmonic of the input current and to improve THD's so that the power level at which the input-current harmonic content still meets the IEC555-2 standard is extended [3]–[6]. Specifically, the approach based on the variable-switching-frequency control was presented and analyzed in [4] and [5]. However, since the switching frequency of these rectifiers directly depends on the input voltage and output power variations, this technique suffers from a very wide-switching-frequency range which decreases the efficiency and makes the rectifier design, device selection, and control circuit more complex.

To improve the performance of the DCM boost rectifier at a constant switching frequency, sixth-harmonic injection methods have been introduced in [3] and [6]. The injected sixth-harmonic signal modifies the duty cycle of the rectifier switch so that the fifth-order harmonic of the input current and the overall THD's are reduced to meet the IEC555-2 requirements. However, if the phase of the injected sixth-harmonic signal is not well synchronized with the fifth-order harmonic of the input current, the expected reduction of the fifth-order harmonic and the improvement of the THD's cannot be achieved. For example, the proposed sixth-harmonic injection circuit in [3], which employs a bandpass filter, has a severe phase-shift problem which requires phase-detecting and phase-locking circuits for reliable operation. In fact, the harmonic-injection technique which utilizes the voltage ripple of the rectifier output voltage and employs phase-detecting and phase-locking circuits to properly synchronize the injected signal with the rectifier input currents is proposed in [6].

In this paper, a robust low-cost harmonic-injection method for the single-switch three-phase DCM boost rectifier and its implementations are presented. To reduce the fifth-order harmonic and improve THD's of the rectifier input currents, a periodic voltage signal is injected to vary the duty cycle of the rectifier within a line cycle. The proposed harmonic-injection technique uses a voltage signal which is proportional

Manuscript received May 1, 1997; revised February 10, 1998. Recommended by Associate Editor, P. Enjeti.

The authors are with the Power Electronics Laboratory, Delta Products Corporation, Research Triangle Park, NC 27709-2173 USA.

Publisher Item Identifier S 0885-8993(98)06471-0.

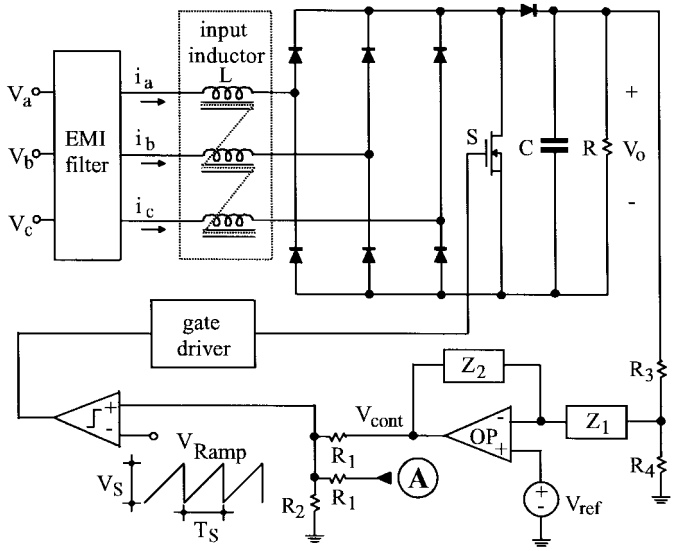


Fig. 1. Conventional single-switch three-phase DCM boost rectifier.

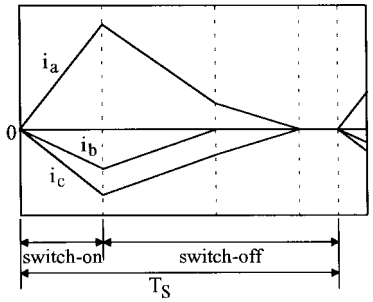


Fig. 2. Input currents $i_a$, $i_b$, and $i_c$ of the conventional single-switch three-phase DCM boost rectifier. The currents are drawn assuming $V_a > 0$ and $V_c < V_b < 0$.

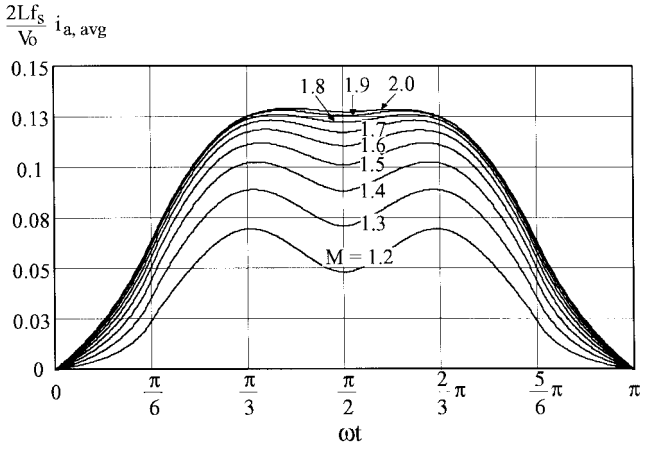


Fig. 3. Normalized average input current $i_{a,\mathrm{avg}}$ of the conventional single-switch three-phase DCM boost rectifier for different voltage-conversion ratios $M$.

to the inverted ac component of the rectified three-phase line-to-line input voltages. As a result, the injected signal is naturally synchronized with the three-phase line-to-neutral input voltages. Moreover, the closed-loop feedback control of the DCM boost rectifier is not affected by the proposed open-loop harmonic-injection method.

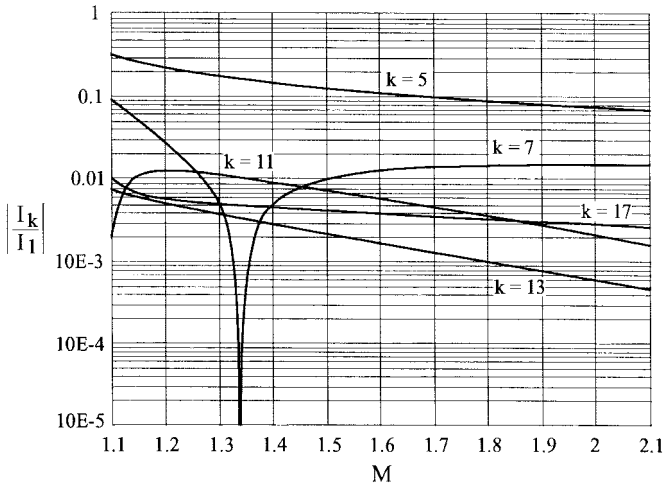


Fig. 4. Normalized input-current harmonics of the single-switch three-phase constant-frequency constant-duty-cycle DCM boost rectifier. Harmonics are normalized with respect to the fundamental component.

## II. Brief Review of Operation and Input-Current Harmonic Analysis of Three-Phase PWM DCM Boost Rectifiers

In this section, a brief review of the operation and input-current harmonic-content analysis of the single-switch three-phase PWM DCM boost rectifier, shown in Fig. 1, is presented, assuming the following.

1) The rectifier operates in DCM.
2) Switching frequency $f_S$ is much higher than line frequency $f_L$.
3) The three-phase input voltages are well-balanced undistorted sinewaves.
4) The input voltage can be considered constant during a switching interval.
5) The output voltage and output current are approximately constant.
6) All semiconductor components are ideal.
7) There are no power losses in the converter.

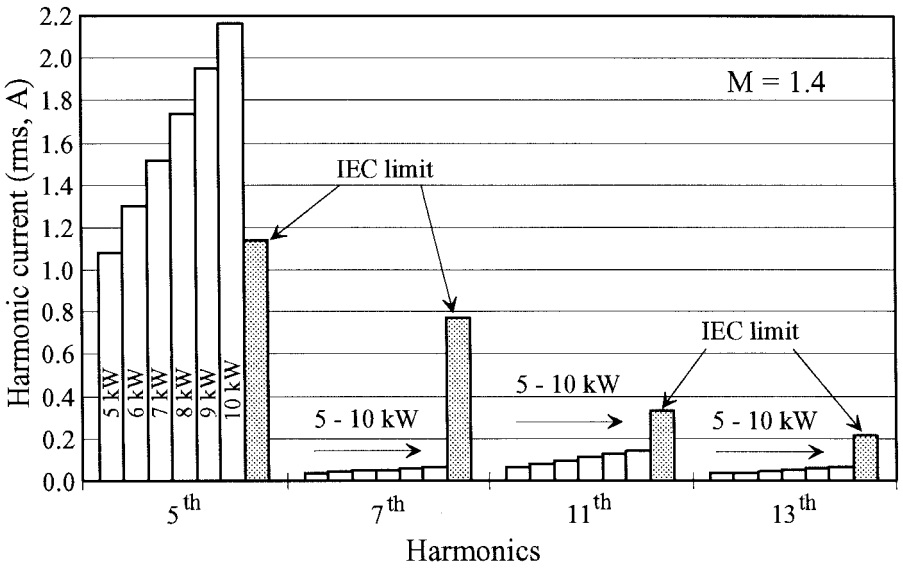


Fig. 5. Comparison between input-current harmonic content of the DCM boost rectifier and harmonic-current limits of the IEC555-2 for $M = 1.4$, $V_{\rm out} = 750$ V, $V_{\rm in(L\text{-}L)} = 380$ $V_{\rm rms}$, and $P_{\rm in} = 5$ to 10 kW.

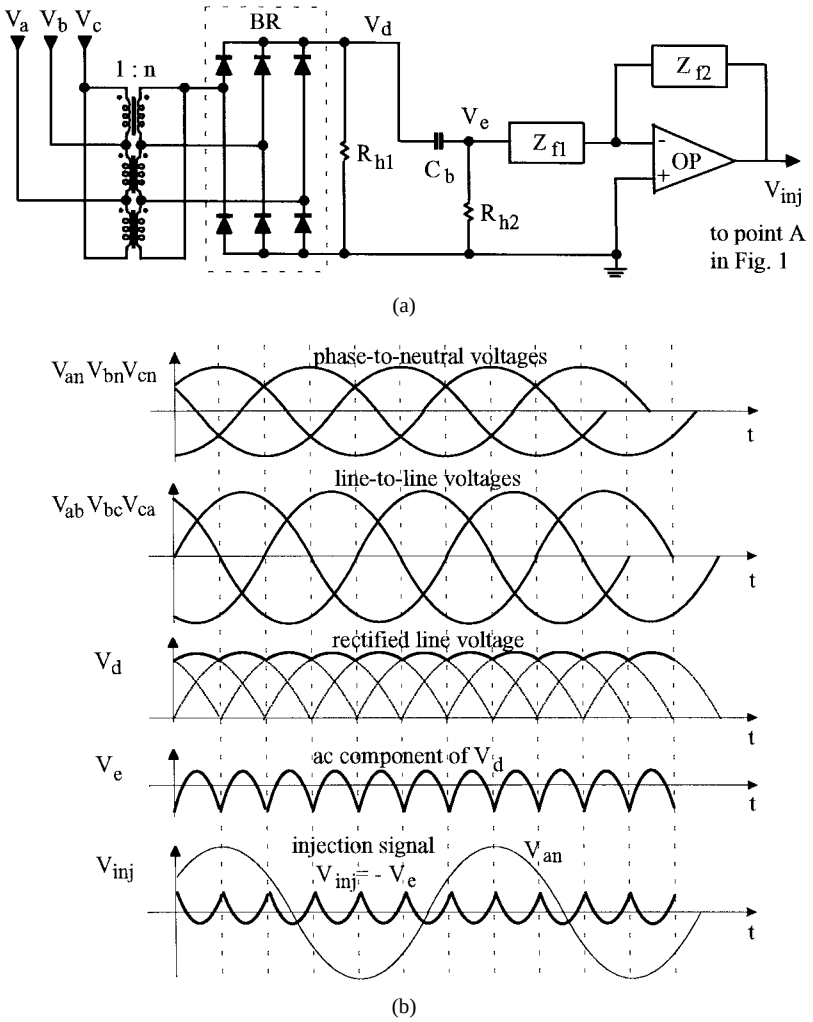


Fig. 6. Injection circuit with isolation transformers: (a) schematic diagram and (b) key voltage waveforms.

Since the boost rectifier is operated in DCM with a constant frequency and constant duty cycle, all three-phase input currents $i_a$, $i_b$, and $i_c$ are zero at the end of a switching period immediately before boost switch $S$ is turned on. After switch $S$ is turned on, $i_a$, $i_b$, and $i_c$ increase linearly to the peak values which are proportional to the line-to-neutral voltages, as shown in Fig. 2. Therefore, during the switch-on period of the rectifier, each line current forms a triangular pulse

with the peak value proportional to the associated line-to-neutral voltage. As a result, during the switch-on period, the average line currents are proportional to the line-to-neutral voltages. When the switch is turned off, the input currents start decreasing because output voltage $V_o$ is higher than the peak of the input voltage. In DCM, the input currents reach zero before the end of the switching period. Since the rate of the input-current decrease is proportional to the difference between output voltage $V_o$ and line-to-neutral voltage, the average line currents during the switch-off period are not proportional to the line voltages, i.e., even if the line voltages are perfectly balanced and sinusoidal, the line currents are distorted.

The average line currents during a switching period of a constant-frequency constant-duty-cycle DCM boost rectifier were derived in [1] and [5]. The derivations assume that switching frequency $f_S$ is much higher than line frequency $f_L$; the well-balanced and undistorted three-phase input voltages can be considered constant within each switching cycle, i.e.,

$$V_a = V_m \sin(\omega t) \tag{1}$$

$$V_b = V_m \sin\left(\omega t - \frac{2\pi}{3}\right) \tag{2}$$

$$V_c = V_m \sin\left(\omega t - \frac{4\pi}{3}\right) \tag{3}$$

where $V_m$ is the peak line-to-neutral voltage and $\omega = 2\pi f_L$ is angular line frequency. According to [1] and [5], the average input currents over a switching period are given by

$$i_{a,\text{avg}} = \frac{V_o D^2}{2Lf_s} \frac{\sin(\omega t)}{\sqrt{3}M - 3\sin(\omega t)} \quad \left(0 \le \omega t \le \frac{\pi}{6}\right) \tag{4}$$

$$i_{a,\text{avg}} = \frac{V_o D^2}{2Lf_s} \frac{M\sin(\omega t) + \frac{1}{2}\sin\left(2\omega t - \frac{2\pi}{3}\right)}{\left[\sqrt{3}M - 3\sin\left(\omega t + \frac{2\pi}{3}\right)\right]\left[M - \sin\left(\omega t + \frac{\pi}{6}\right)\right]} \quad \left(\frac{\pi}{6} \le \omega t \le \frac{\pi}{3}\right) \tag{5}$$

$$i_{a,\text{avg}} = \frac{V_o D^2}{2Lf_s} \frac{M\sin(\omega t) + \sin\left(2\omega t + \frac{\pi}{3}\right)}{\left[\sqrt{3}M + 3\sin\left(\omega t + \frac{2\pi}{3}\right)\right]\left[M - \sin\left(\omega t + \frac{\pi}{6}\right)\right]} \quad \left(\frac{\pi}{3} \le \omega t \le \frac{\pi}{2}\right) \tag{6}$$

where $V_o$ is the rectifier output voltage, $D$ is the duty ratio, $L$ is the inductance of the input inductors, and $M$ is the voltage conversion ratio defined as

$$M = \frac{V_o}{\sqrt{3}V_m}. \tag{7}$$

From (4) to (7), the average input currents for different voltage-conversion ratios are calculated and plotted as shown in Fig. 3. The THD's and harmonic contents of the average input current for different values of $M$ can be calculated by Fourier analysis. Fig. 4 shows the normalized harmonic content of the rectifier input current as a function of $M$, whose practical range is from 1.2 to 2. As can be seen from Fig. 4, the rectifier input-current spectrum which contains only odd harmonics is dominated by the fifth-order harmonic, i.e., the lowest order harmonic. For example, at $M = 1.2$, the fifth-order harmonic is eight times larger than the seventh-order harmonic which is the next largest. Also, it should be noted that the value of the normalized fifth-order harmonic monotonically decreases as the values of $M$ increase. In fact, it decreases from slightly over 40% of the fundamental component at $M = 1.1$ to approximately 7% at $M = 2$.

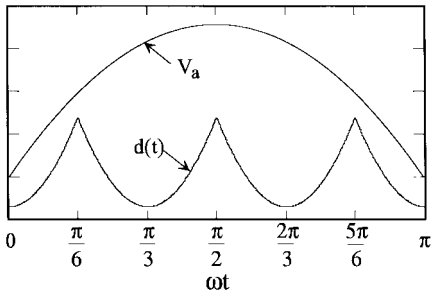


Fig. 7. Duty-cycle variations during a half of the fundamental line period.

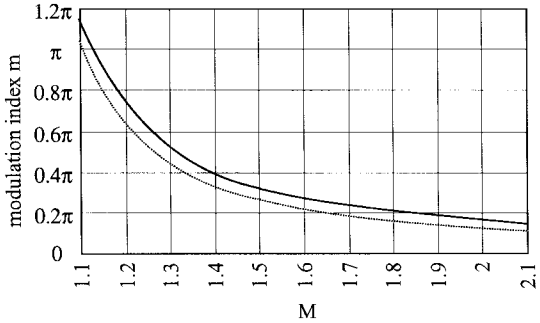


Fig. 8. Optimal modulation index $m$ versus voltage conversion ratio $M$ for the minimum THD's (solid line) and for the maximum output power (dashed line).

Generally, the maximum input power at which the three-phase constant-frequency DCM boost rectifier can meet the IEC555-2 specifications is limited by the fifth-order harmonic of the input current. As an illustration, Fig. 5 shows the fifth, seventh, eleventh, and thirteenth harmonics of the DCM boost rectifier with $M = 1.4$ and input power levels from 5 to 10 kW, along with the corresponding IEC555-2 limits. As can be seen from Fig. 5, for $M = 1.4$, the rectifier can meet the IEC555-2 requirements only for power levels up to 5 kW because of the fifth-harmonic limitation. The higher order harmonics, i.e., seventh, eleventh, thirteenth, etc., are well below the IEC555-2 limits, even for power levels over 10 kW.

To meet the IEC555-2 specifications at power levels above 5 kW, the three-phase constant-frequency constant-duty-cycle DCM boost rectifier needs to be designed with a higher $M$ [3]. However, it should be noted that for a given power line voltage, larger $M$ requires a boost switch with a higher voltage rating. Therefore, to maximize the efficiency and reduce the cost, the design with the minimum $M$ which meets the specifications such as IEC555-2 or desired THD's should be used.

Since the fifth-order harmonic is the dominant harmonic in the input-current spectrums, as shown in Fig. 4, the three-phase input currents of the constant-switching-frequency constant-duty-ratio DCM boost rectifier can be approximated

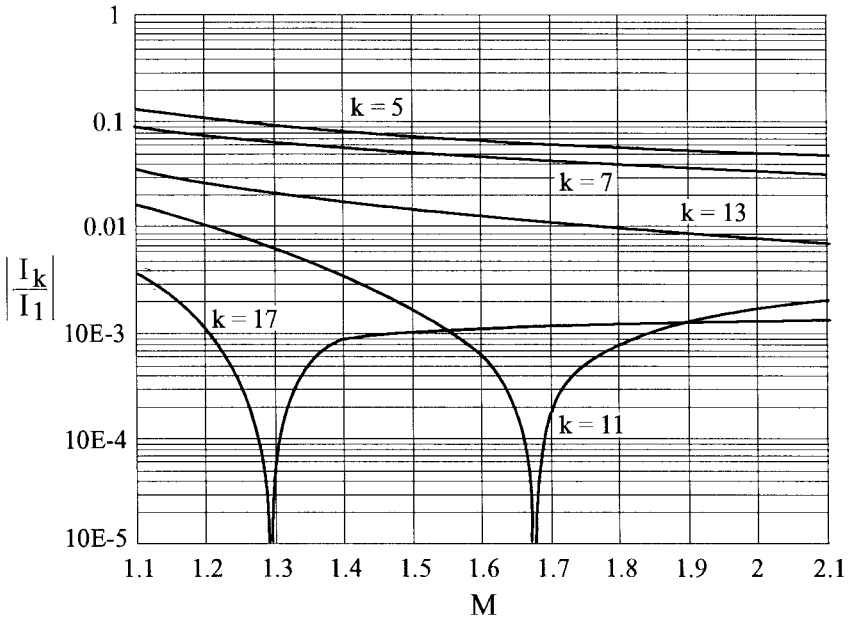


Fig. 9. Normalized input-current harmonics of the single-switch three-phase DCM boost rectifier with the proposed harmonic-injection control. Harmonics are normalized with respect to the fundamental component.

by neglecting the higher order harmonics as

$$i_{a,\text{avg}} = I_1 \sin(\omega t) - I_5 \sin(5\omega t) \tag{8}$$

$$i_{b,\text{avg}} = I_1 \sin\left(\omega t - \frac{2\pi}{3}\right) - I_5 \sin\left(5\omega t - \frac{2\pi}{3}\right) \tag{9}$$

$$i_{c,\text{avg}} = I_1 \sin\left(\omega t - \frac{4\pi}{3}\right) - I_5 \sin\left(5\omega t - \frac{4\pi}{3}\right). \tag{10}$$

## III. New Low-Cost Injection-Signal Generators

In the circuit proposed in this paper, a signal proportional to the inverted ac component of the three-phase line-to-line input voltages is injected into the control circuit at node A in Fig. 1 to modulate the duty cycle of the boost rectifier switch and reduce the fifth-order harmonic of the line current. Two implementations of the injection-signal generator are described in this paper. One implementation uses three low-frequency step-down transformers to generate the injection signal; the other implementation does not require the transformers, but instead employs operational amplifiers (opamps) to accomplish the same task.

### *A. Implementation with Transformers*

The circuit diagram of the injection-signal generator implemented with three low-frequency step-down transformers, along with its key waveforms, is shown in Fig. 6. Besides the three transformers, the circuit in Fig. 6(a) also incorporates three-phase diode bridge BR, blocking capacitor $C_b$, and an opamp with a feedback network ($Z_{f1}$ and $Z_{f2}$). Three low-frequency transformers are utilized for the voltage step-down and isolation between the injection circuit and the power stage. The primary terminals of the step-down transformers are connected to the line-to-line input voltages $V_{ab}$, $V_{bc}$, and $V_{ca}$. The secondary-side voltages of the transformers are rectified by three-phase diode bridge BR. The dc component of rectified voltage $V_d$ is eliminated by blocking capacitor $C_b$. Since the impedance of $C_b$ at the line frequency is much smaller than $R_{h2}$, the voltage across $R_{h2}$ is nearly identical to the ac component of $V_d$. Finally, the polarity of the voltage signal $V_e$ is inverted by the opamp so that the desired injection signal $V_{\text{inj}}$, shown in Fig. 6(b), is obtained.

Since the proposed injection-signal generator does not contain a bandpass filter, but only a high-pass filter with the corner frequency well below the frequency of the sixth-order harmonic, the injection signal which contains sixth-order and higher order harmonics does not suffer from any significant delay. As a result, the injection signal $V_{\text{inj}}$ phase is naturally well synchronized with all the input currents and line-to-neutral voltages. Moreover, this phase synchronization does not drift with time, and it is not very sensitive to component tolerances.

When signal $V_{\text{inj}}$, shown in Fig. 6(b), is injected at the input of the PWM modulator (node A in Fig. 1), it modifies the duty cycle so that the fifth-order harmonic of the input current is reduced and the THD's are improved. In fact, since the variation of duty cycle $d(t)$ is directly proportional to the injected signal $V_{\text{inj}}$, the modulation of duty ratio during a line cycle can be described as

$$D_{\text{MOD}}(t) = D[1 + d(t)] \tag{11}$$

where $D_{\text{MOD}}$ is the modulated duty cycle, $D$ is the duty cycle in the absence of the modulation, and $d(t)$ is the duty cycle modulation. Since $d(t)$ is proportional to the inverted ac component of the rectified three-phase line-to-line input voltages, the variation of duty cycle $d(t)$ during a half of the fundamental line period can be plotted along with the line-to-neutral input voltage, as shown in Fig. 7. Moreover, $d(t)$ can be described as a function of modulation factor $m$ and angular line frequency $\omega t$ for the first quarter of the fundamental period

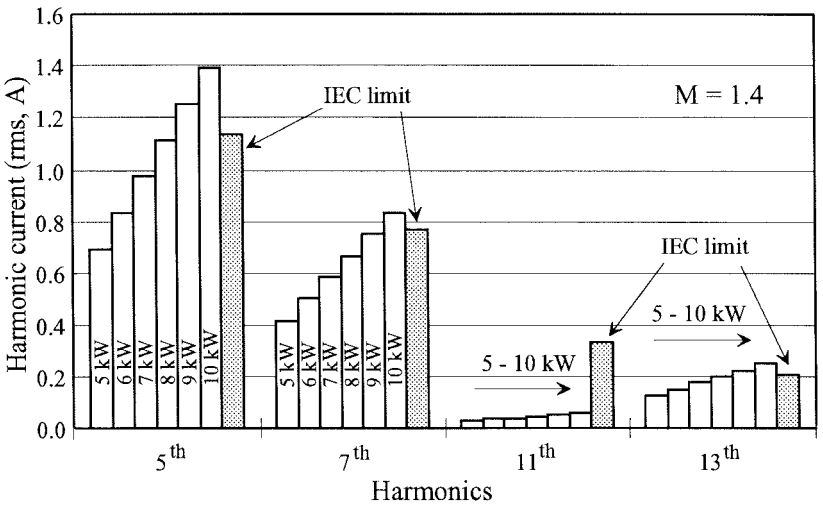


Fig. 10. Comparison between input-current harmonic content of the DCM boost rectifier with the proposed harmonic injection and harmonic-current limits of the IEC555-2 for $M = 1.4$, $V_{\rm out} = 750$ V, $V_{\rm in(L\text{-}L)} = 380$ $V_{\rm rms}$, and $P_{\rm in} = 5$ to 10 kW.

$(0 < \omega t < \pi/2)$ as

$$d(t) = -m\left[\cos(\omega t) - \frac{6}{\pi}\cos\frac{\pi}{3}\right] \quad \left(0 \le \omega t \le \frac{\pi}{6}\right) \tag{12}$$

$$d(t) = -m\left[\cos\left(\omega t - \frac{\pi}{3}\right) - \frac{6}{\pi}\cos\frac{\pi}{3}\right] \quad \left(\frac{\pi}{6} \le \omega t \le \frac{\pi}{2}\right) \tag{13}$$

where $m$ is the modulation factor defined as

$$m = \sqrt{3}V_m \times n \times \frac{Z_{f2}}{Z_{f1}} \times \frac{1}{V_{\rm cont}}. \tag{14}$$

As shown in Fig. 6, $n$ is the transformer turns ratio and $Z_{f2}/Z_{f1}$ is the feedback gain of the opamp, while $V_m$ is the peak line-to-neutral input voltage, and $V_{\rm cont}$ is the output voltage of the gain compensator shown in Fig. 1. It should be noted that the expressions for $d(t)$ given in (12) and (13) are valid for a quarter of the fundamental period $(0 < \omega t < \pi/2)$. However, they can be easily extended to a whole line period because of the waveform symmetry.

The periodic function described by (12) and (13) can be expressed in terms of the Fourier series representation as

$$d(t) = \frac{m}{\pi}\sum_{n=1}^{\infty}\frac{(-1)^n 6}{(6n)^2 - 1}\cos(6n\omega t). \tag{15}$$

From (15), it can be seen that the generated injection signal contains not only the sixth-order harmonic, but also higher order harmonics such as 12th, 18th, etc. These higher order harmonics help improve THD's more than if only the sixth-order harmonic is injected.

By substituting $D$ in (4)–(6) with the modified duty ratio $D_{\rm MOD}$ defined in (11), the average input current $i_{a,\rm avg}^{\rm inj}$ in the presence of the signal injection can be described as

$$i_{a,\rm avg}^{\rm inj} = i_{a,\rm avg}(1 + d(t))^2 \approx i_{a,\rm avg}(1 + 2d(t)) \tag{16}$$

where $d(t)^2$ term is neglected, since it is much smaller than the unity. Using (8) and (15), the average input current $i_{a,\rm avg}^{\rm inj}$ defined in (16) can be calculated as

$$\begin{aligned} i_{a,\rm avg}^{\rm inj} = {} & (I_1 - qI_5)\sin(\omega t) - (I_5 - qI_1)\sin(5\omega t) \\ & - \left(qI_1 - \frac{35}{143}qI_5\right)\sin(7\omega t) \\ & + \left(qI_5 - \frac{35}{143}qI_1\right)\sin(11\omega t) \\ & + \left(\frac{35}{143}qI_1 - \frac{35}{323}qI_5\right)\sin(13\omega t)\cdots \end{aligned} \tag{17}$$

where the constant $q$ is defined as

$$q = \frac{6}{35\pi}m \tag{18}$$

i.e., it is proportional to modulation index $m$.

Similarly, the input currents $i_{b,\rm avg}^{\rm inj}$ and $i_{c,\rm avg}^{\rm inj}$ can also be calculated as

$$\begin{aligned} i_{b,\rm avg}^{\rm inj} = {} & (I_1 - qI_5)\sin\left(\omega t - \frac{2\pi}{3}\right) \\ & + (I_5 - qI_1)\sin\left(5\omega t + \frac{\pi}{3}\right) \\ & + \left(qI_1 - \frac{35}{143}qI_5\right)\sin\left(7\omega t + \frac{\pi}{3}\right) \\ & + \left(qI_5 - \frac{35}{143}qI_1\right)\sin\left(11\omega t - \frac{2\pi}{3}\right)\cdots \end{aligned} \tag{19}$$

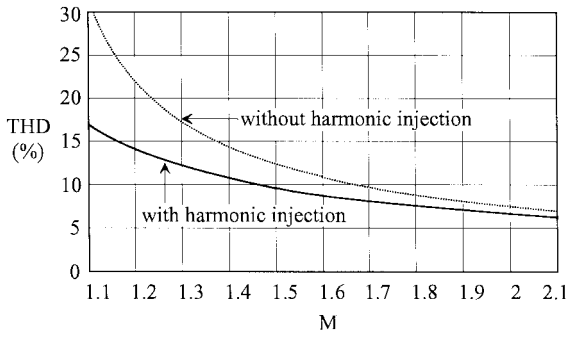


Fig. 11. Input-current THD's as functions of the voltage-conversion ratio of a constant-frequency DCM boost rectifier with constant duty cycle (dashed line) and with modulated duty cycle using the proposed harmonic-injection method (solid line).

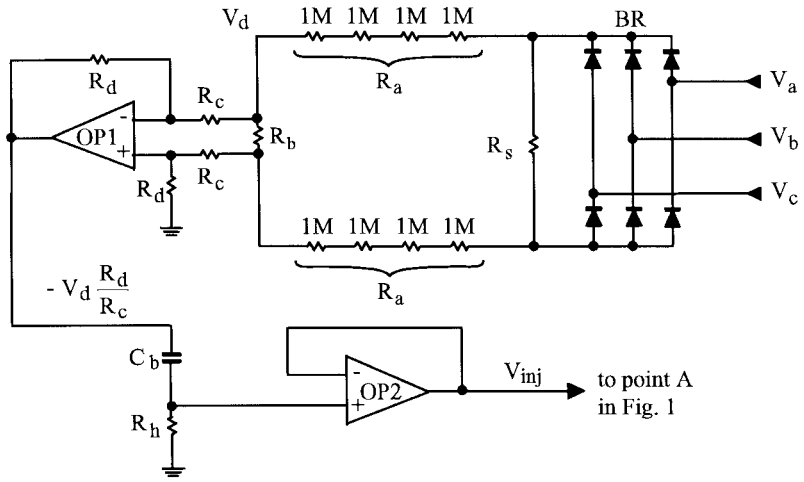


Fig. 12. Schematic diagram of the harmonic-injection circuit with a difference opamp. The key circuit waveforms are the same as in Fig. 6(b).

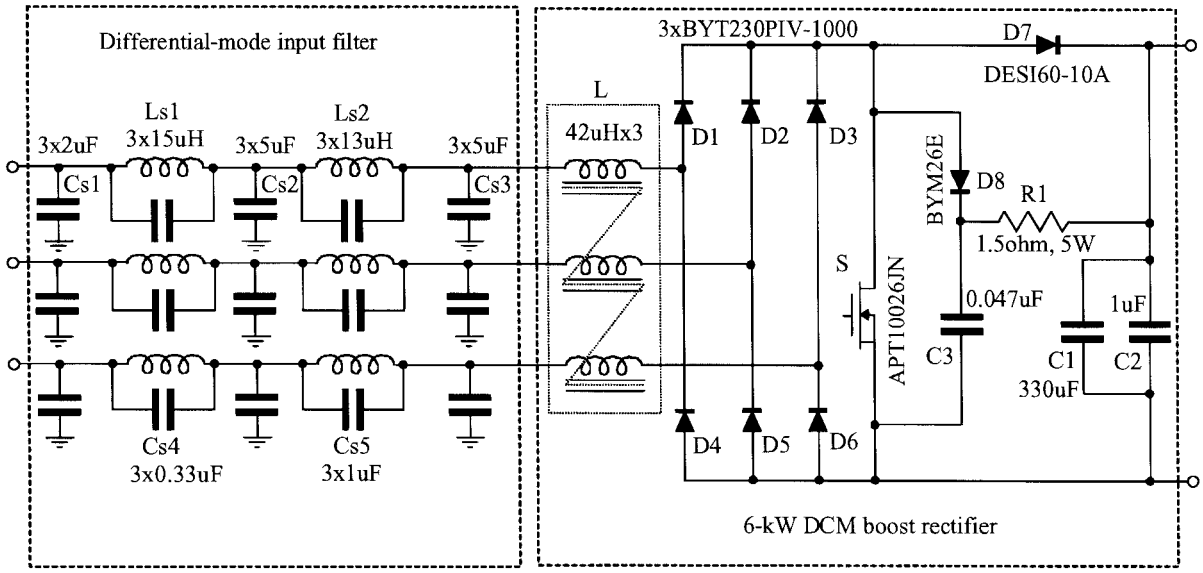


Fig. 13. Schematic diagram of the 6-kW single-switch 3-$\phi$ DCM boost rectifier.

$$i_{c,\text{avg}}^{\text{inj}} = (I_1 - qI_5)\sin\left(\omega t - \frac{4\pi}{3}\right) + (I_5 - qI_1)\sin\left(5\omega t - \frac{\pi}{3}\right) + \left(qI_1 - \frac{35}{143}qI_5\right)\sin\left(7\omega t - \frac{\pi}{3}\right) + \left(qI_5 - \frac{35}{143}qI_1\right)\sin\left(11\omega t - \frac{4\pi}{3}\right)\cdots. \quad (20)$$

Therefore, from (17) to (20), the THD's of the input currents of the three-phase constant-frequency DCM boost rectifier with the proposed harmonic-injection control is given by

$$\text{THD's} = \frac{\sqrt{(I_5 - qI_1)^2 + \left(qI_1 - \frac{35}{143}qI_5\right)^2 + \left(qI_5 - \frac{35}{143}qI_1\right)^2\cdots}}{I_1 - qI_5}. \quad (21)$$

From (17) to (21), it can be seen that for a given voltage conversion ratio, the THD's are a function of modulation index $m$.

At any given voltage-conversion ratio $M$, optimal modulation index $m$, which produces the minimum THD's, can be determined from (18) and (21). Fig. 8 shows the calculated values of optimal modulation index $m$ for the minimum THD's (solid line) as a function of $M$. To maximize the input power of the rectifier at which the IEC555-2 specifications are met, modulation index $m$ should be determined so that the ratio of the seventh-order harmonic and the fifth-order harmonic is equal to corresponding IEC555-2 limits, i.e.,

$$\left|\frac{qI_1 - \frac{35}{143}qI_5}{I_5 - qI_1}\right| = \frac{0.77\text{ A}}{1.14\text{ A}} = 0.675 \quad (22)$$

where 1.14 and 0.77 A are IEC555-2 limits for the fifth- and seventh-order harmonics, respectively. It should be noted that the effects of the higher order harmonics are not significant in comparison with the fifth- and seventh-order harmonics.

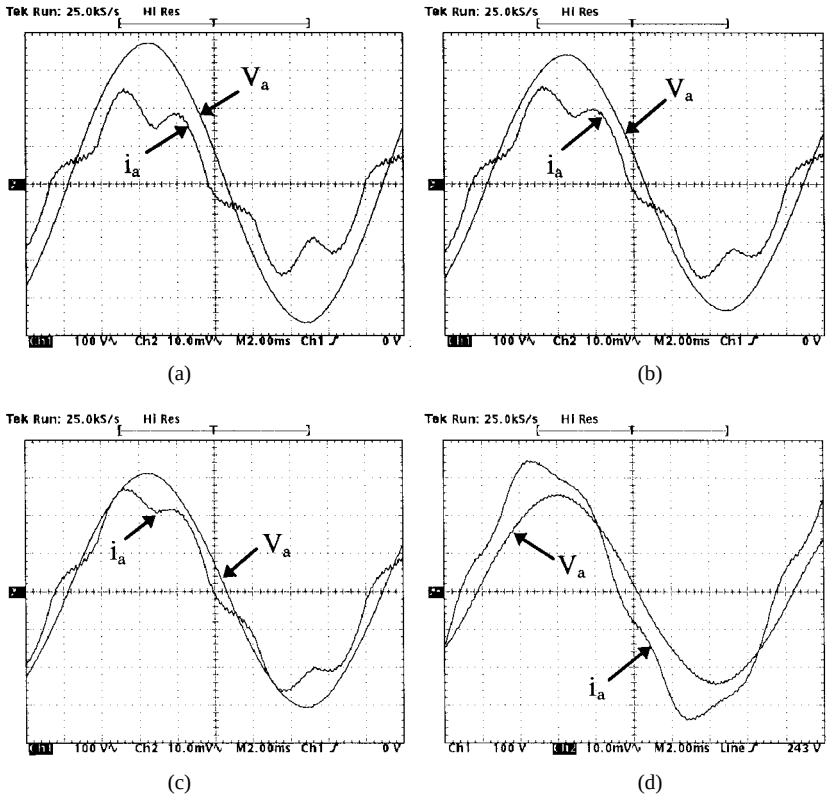


Fig. 14. Input voltage $V_a$ (100 V/div) and input current $i_a$ (5 A/div) waveforms of the experimental 6-kW DCM boost rectifier without harmonic-injection control at: (a) $V_{\mathrm{in(LL)}} = 456\ \mathrm{V_{rms}}$, (b) 417 $\mathrm{V_{rms}}$, (c) 380 $\mathrm{V_{rms}}$, and (d) 304 $\mathrm{V_{rms}}$.

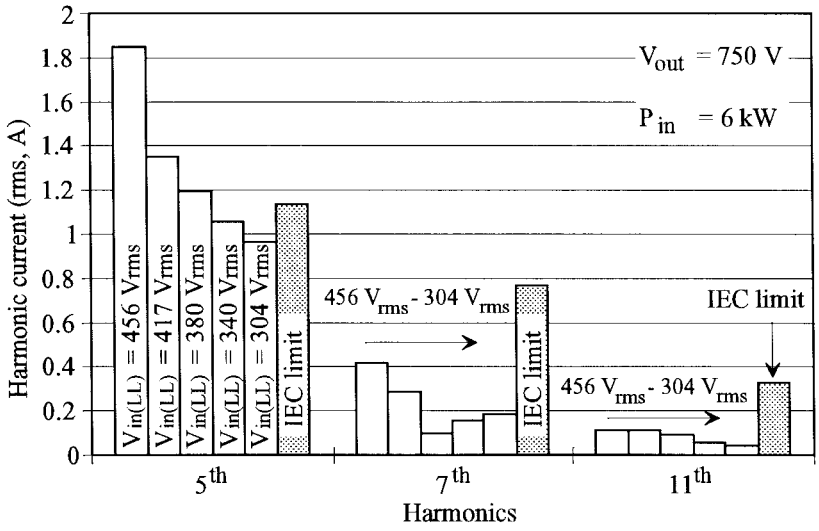


Fig. 15. Measured full-power input-current harmonics of the experimental DCM boost rectifier without harmonic-injection control at different input voltages.

Moreover, the higher frequency harmonics can be easily eliminated by an electromagnetic interference (EMI) input filter. Fig. 8 shows the calculated values of optimal modulation index $m$ for the maximum input power (dashed line) as a function of $M$.

Using the optimal modulation index $m$ for the maximum input power, a normalized harmonic content of the rectifier input current can be calculated as shown in Fig. 9. It can be seen that the magnitudes of the fifth, seventh, and thirteenth harmonics are linearly proportional to one another.

Fig. 10 shows the estimated normalized fifth, seventh, eleventh, and thirteenth harmonics of the input current of the DCM boost rectifier with harmonic-injection control for input power levels from 5 to 10 kW. The harmonics are obtained by assuming that line-to-line input voltage $V_{\mathrm{in(LL)}} = 380\ \mathrm{V_{rms}}$ and output voltage $V_o = 750\ \mathrm{V_{dc}}$, i.e., assuming $M = V_o/(\sqrt{3}V_m) = 1.4$. The IEC555-2 limits for each of the harmonics are also shown in Fig. 10. As can be seen from Fig. 10, employing the proposed injection method, the maximum power of the rectifier at which the IEC555-2

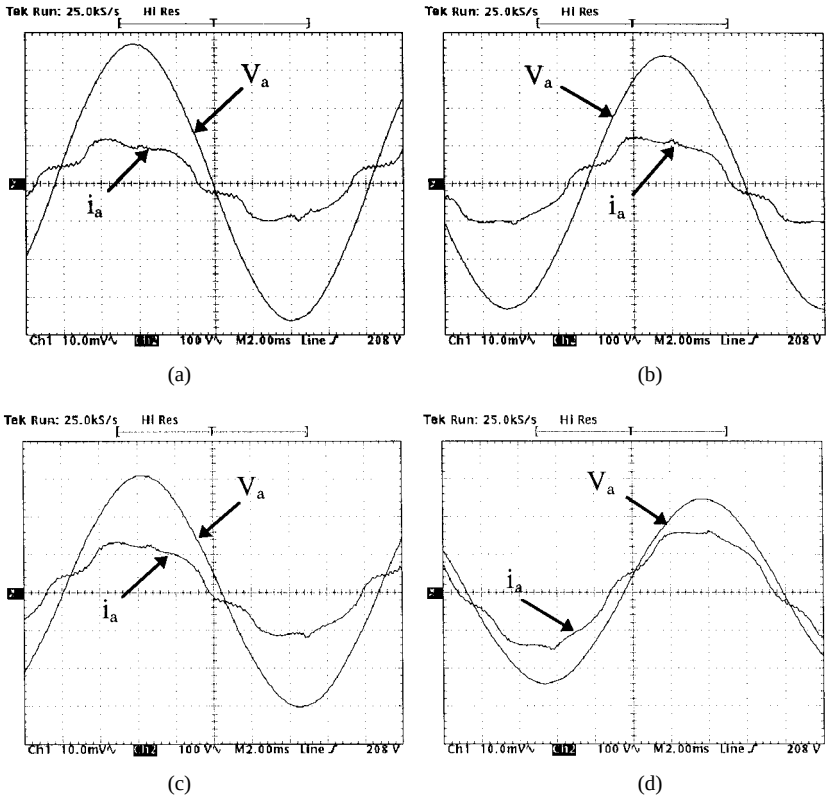


Fig. 16. Input voltage $V_a$ (100 V/div) and input current $i_a$ (10 A/div) waveforms of the experimental 6-kW DCM boost rectifier with the proposed harmonic-injection control at: (a) $V_{\mathrm{in(LL)}} = 456\ \mathrm{V_{rms}}$, (b) 417 $\mathrm{V_{rms}}$, (c) 380 $\mathrm{V_{rms}}$, and (d) 304 $\mathrm{V_{rms}}$.

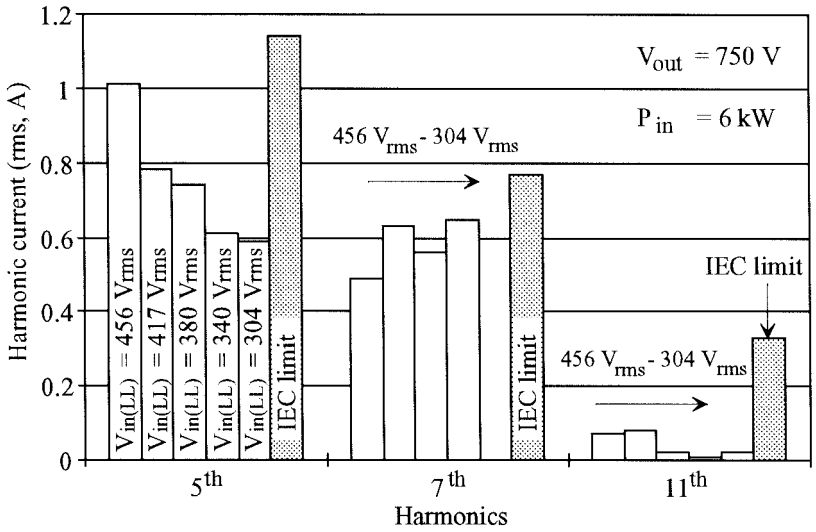


Fig. 17. Measured full-power input-current harmonics of the experimental DCM boost rectifier with harmonic-injection control at different input voltages.

requirements are met is extended to 8 kW. As shown in Fig. 5, the corresponding maximum power for the rectifier without harmonic injection at $M = 1.4$ is only about 5 kW.

Finally, the comparison between the THD's of the constant-switching-frequency, DCM boost rectifier without and with the proposed harmonic injection is given in Fig. 11. As can be seen from Fig. 11, the reduction of the THD's with the proposed injection technique is the most significant for $M < 1.4$. Specifically, for $M < 1.4$, the reduction in the THD's is at least 5%. For larger values of $M$, the injection approach is less effective. For example, for $M = 2$, the reduction of the THD's of the circuit with the injection is less than 1% in comparison with that without the injection.

### *B. Implementation Without Transformers*

The injection signal generator can also be implemented without the bulky low-frequency step-down transformers, as shown in Fig. 12. In the implementation in Fig. 12, the three-

TABLE I
MEASURED INPUT-CURRENT HARMONICS OF THE EXPERIMENTAL 6-kW DCM BOOST RECTIFIER WITH THE HARMONIC-INJECTION CONTROL AT FULL POWER AND DIFFERENT INPUT VOLTAGES

| harmonic number | three-phase input voltages | | | | | IEC555-2 limits |
|---|---|---|---|---|---|---|
| | 456 $V_{rms(LL)}$ | 417 $V_{rms(LL)}$ | 380 $V_{rms(LL)}$ | 340 $V_{rms(LL)}$ | 304 $V_{rms(LL)}$ | |
| 1 | 7.72 A | 8.4 A | 9.19 A | 10.28 A | 11.3 A | |
| 3 | 0.12 A | 0.12 A | 0.08 A | 0.09 A | 0.06 A | 2.3 A |
| 5 | 1.01 A | 0.78 A | 0.74 A | 0.61 A | 0.59 A | 1.14 A |
| 7 | 0.49 A | 0.63 A | 0.56 A | 0.65 A | 0.60 A | 0.77 A |
| 9 | 0.04 A | 0.02 A | 0.02 A | 0.01 A | 0.02 A | 0.4 A |
| 11 | 0.07 A | 0.08 A | 0.02 A | 0.01 A | 0.02 A | 0.33 A |
| 2 | 0.18 A | 0.15 A | 0.13 A | 0.12 A | 0.11 A | 1.08 A |
| 4 | 0.22 A | 0.2 A | 0.17 A | 0.16 A | 0.14 A | 0.43 A |
| 6 | 0.01 A | 0.01 A | 0.00 A | 0.01 A | 0.01 A | 0.3 A |
| 8 | 0.01 A | 0.04 A | 0.01 A | 0.02 A | 0.01 A | 0.23 A |
| 10 | 0.05 A | 0.01 A | 0.03 A | 0.01 A | 0.01 A | 0.184 A |
| THDs | 15.74% | 12.86% | 10.93% | 9.23% | 7.52% | |

TABLE II
MEASURED FULL-POWER EFFICIENCY OF THE EXPERIMENTAL 6-kW DCM BOOST RECTIFIER WITH THE PROPOSED HARMONIC-INJECTION CONTROL AT DIFFERENT INPUT VOLTAGES

| input voltage [V] | input power [W] | output voltage [V] | output power [W] | loss [W] | efficiency [%] |
|---|---|---|---|---|---|
| 456 | 5870 | 752 | 5759 | 111 | 98.1 |
| 417 | 5910 | 752 | 5772 | 138 | 97.7 |
| 380 | 5983 | 755 | 5815 | 168 | 97.2 |
| 340 | 5956 | 752 | 5756 | 200 | 96.6 |
| 304 | 5975 | 750 | 5740 | 235 | 96.1 |

* Input and output power measurements: Voltech PM3000A Universal Power Analyzer, PM1000 AC Power Analyzer

phase line voltage is first rectified by three-phase bridge rectifier BR and then attenuated by resistive voltage divider $R_a - R_b$. The scaled-down line voltage developed across $R_b$ is then inverted by difference amplifier OP1 which is referenced to the control ground. It should be noted that the control ground is isolated from the ground of three-phase input voltages by $R_a = 4$ MΩ resistors. The dc component of the output voltage of difference amplifier OP1 is eliminated by blocking capacitor $C_b$. Since the impedance of blocking capacitor $C_b$ at the line frequency is much smaller than $R_h$, the voltage across $R_h$ which is desired signal $V_{\rm inj}$ is nearly identical to the ac component of the output voltage of difference amplifier OP1. Finally, $V_{\rm inj}$ is injected in the circuit in Fig. 1 at point A through a buffer, OP2. As in the case of the implementation with the transformers, voltage signal $V_{\rm inj}$ is naturally in phase with all input currents and line-to-neutral voltages. The performance of the circuit in Fig. 12 is identical to that of the circuit in Fig. 6. However, the injection circuit shown in Fig. 12 has a smaller size and is less expensive than the circuit shown in Fig. 6.

## IV. EXPERIMENTAL RESULTS

To verify the performance of the proposed injection technique, a three-phase 6-kW DCM boost rectifier for the 304–456-$V_{\rm rms}$ line-to-line input voltage range (380 $V_{\rm rms}$ ±20%) and $V_o = 750$ $V_{\rm dc}$ was built. The circuit diagram of the power stage is given in Fig. 13. The rectifier was designed with a constant switching frequency of 45 kHz.

Fig. 14 shows the oscillograms of input voltage and current waveforms of the experimental circuit without harmonic-injection control at full power and different input voltages, while Fig. 15 shows the measured input-current harmonics under the same conditions. As can be seen from Fig. 15, the fifth-order harmonic of the input current is over the IEC555-2 limit for the nominal input voltage (380 $V_{\rm rms}$) and higher.

To evaluate the performance of the proposed injection approach, both implementations of the injection circuit (with and without step-down transformers), shown in Figs. 6(a) and 12, were built. Fig. 16 shows the oscillograms of input voltage and current waveforms of the experimental circuit with harmonic-injection control at full power and different input voltages.

The measured input-current harmonics of the experimental rectifier at full power and at different input voltages are summarized in Fig. 17. It should be noted that the measured performances of both implementations were also identical. As can be seen from Fig. 17, the magnitudes of the fifth-order harmonic as well as the higher harmonics are well below the IEC555-2 limit in the entire input voltage range (304–456 $V_{\rm rms}$).

Finally, Table I shows the measured rms input-current harmonics at different input voltages, while Table II shows the full-power measured efficiency of the rectifier at the same range of input voltages. The rectifier exhibits the maximum efficiency of 98% at the maximum input voltage of 456 $V_{\rm rms}$.

The minimum efficiency of 96% occurs at lower line (304 $V_{rms}$).

## V. Conclusion

In this paper, a new robust low-cost harmonic-injection method for single-switch three-phase DCM boost rectifiers has been described. In the proposed method, a periodic voltage which is proportional to the inverted ac component of the rectified three-phase line-to-line input voltages is injected in the control circuit to vary the duty cycle of the rectifier switch within a line cycle so that the fifth-order harmonic of the input current is reduced to meet the IEC555-2 requirement. Moreover, the injected duty-cycle variations are naturally synchronized with the three-phase line-to-neutral input voltages without using expensive phase-detecting and phase-locking circuits. The analysis of the injected signal and modified harmonic currents of the rectifier has been presented and verified on a laboratory prototype. The measured input-current harmonics of the 6-kW prototype rectifier were found to be well below the IEC555-2 limits over the entire input voltage range (304–456 $V_{rms}$). The rectifier efficiency is about 97% at full load and nominal line.

## References

[1] A. R. Prasad, P. D. Ziogas, and S. Manias, "An active power factor correction technique for three-phase diode rectifiers," in *IEEE Power Electronics Specialists Conf. (PESC) Rec.*, 1989, pp. 58–66.

[2] International Electrotechnical Commission, Sub-Committee 77A, "Equipment connection to the public low-voltage supply system," Draft Revision of IEC555-2: "Harmonic," Budapest, Hungary, Oct. 1990.

[3] Q. Huang and F. C. Lee, "Harmonic reduction in a single-switch, three-phase boost rectifier with high order harmonic injected PWM," in *IEEE Power Electronics Specialists Conf. (PESC) Rec.*, 1996, pp. 1266–1271.

[4] L. Simonetti, J. Sebastian, and J. Uceda, "Single-switch three-phase power factor under variable switching frequency and discontinuous input current," in *IEEE Power Electronics Specialists Conf. (PESC) Rec.*, 1993, pp. 657–662.

[5] J. W. Kolar, H. Ertl, and F. C. Zach, "Space vector-based analytical analysis of the input current distortion of a three-phase discontinuous-mode boost rectifier system," in *IEEE Power Electronics Specialists Conf. (PESC) Rec.*, 1993, pp. 696–703.

[6] J. Sun, N. Fröhleke, and H. Grotstollen, "Harmonic reduction techniques for single-switch three-phase boost rectifiers," in *Conf. Rec. 1996 IEEE Industry Applications Society Annu. Meet.*, 1996, pp. 1225–1232.

**Yungtaek Jang** (S'92–M'95) was born in Seoul, Korea. He received the B.S. degree from Yonsei University, Seoul, in 1982 and the M.S. and Ph.D. degrees from the University of Colorado, Boulder, in 1991 and 1995, respectively, all in electrical engineering.

From 1982 to 1988, he was a Design Engineer at Hyundai Engineering Corporation, Seoul. From 1995 to 1996, he was a Senior Engineer at Advanced Energy Industries, Inc., Fort Collins, CO. He is the Senior Design Engineer at the Power Electronics Laboratory, Delta Products Corporation, Research Triangle Park, NC. His research interests include resonant power conversion, converter modeling, control techniques, and low-harmonic rectification.

**Milan M. Jovanović** (S'86–M'89–SM'89) was born in Belgrade, Yugoslavia. He received the Dipl. Ing. degree in electrical engineering from the University of Belgrade, the M.S.E.E. degree from the University of Novi Sad, Novi Sad, Yugoslavia, and the Ph.D. degree in electrical engineering from the Virginia Polytechnic Institute and State University (Virginia Tech), Blacksburg.

He is the Director of Research and Development of the Power Electronics Laboratory, Delta Products Corporation, Research Triangle Park, NC, the Advanced R&D unit of Delta Electronics, Inc., Taiwan, one of the world's largest manufacturers of power supplies. His 22-year experience includes the analysis and design of high-frequency high-power-density power processors; modeling, testing, evaluation, and application of high-power semiconductor devices; analysis and design of magnetic devices; and modeling, analysis, and design of analog electronics circuits. His current research is focused on power conversion and management issues for portable data-processing equipment, design optimization methods for low-voltage power supplies, distributed power systems, power-factor-correction techniques, and design optimization issues related to the Energy Star ("green power") requirements for desktop-computer power supplies.